

Transformed Poisson–Boltzmann Relations and Ionic Distributions[†]Hong Qian[‡]

Department of Applied Mathematics, University of Washington, Seattle, Washington 98195

John A. Schellman*

Institute of Molecular Biology, University of Oregon, Eugene, Oregon 97403

Received: November 23, 1999; In Final Form: February 24, 2000

For many applications, charge distributions around macromolecules in aqueous solution are of greater interest than the electrical potential. We show that it is possible to use the Poisson–Boltzmann (PB) relation to develop differential equations for the ionic distributions. The solutions to these equations are the integral distribution functions whose derivatives give the charge density functions for counterions and coions. In this formalism the salt-free atmosphere of a cylindrical polyelectrolyte is very easily solvable for the counterion. Quantities such as the “condensation radius” (Le Bret, M.; Zimm, B. H. *Biopolymers* **1984**, 23, 287–312) and the “Bjerrum association radius” (Bjerrum, N. Investigations on Association of Ions, I. In *Niels Bjerrum Selected Papers*; Munksgaard: Copenhagen, 1926; pp 108–19) appear naturally as inflection points in curves of the counterion distribution functions. Moreover, a number of the properties of condensation theory arise as scaling limits of the transformed PB equation. In the presence of added salt separate equations can be derived for the excess charge distributions of counterions and coions. In this case the total excesses of counterion φ_{ct} and of coion φ_{co} are simply related to experiment. Various combinations of these two quantities lead to formulas for (1) the total charge, (2) Donnan exclusion, (3) counterion release (Record, M. T.; Lohman, T. M.; de Haseth, P. J. *Mol. Biol.* **1976**, 107, 145–158), and (4) fraction of “condensed” ions. Bjerrum’s theory of ion association and Manning’s theory of counterion condensation are discussed in the context of the transformed Poisson–Boltzmann theory.

Electrostatic interactions play important roles in chemistry and biology. In biochemistry, interactions between macromolecules often involve charged polyelectrolytes such as proteins and nucleic acids. The interactions are intimately related to the ionic distributions around the macromolecular polyelectrolytes in aqueous solution. A quantitative description of the ionic distributions can be derived from the Poisson–Boltzmann (PB) equation. (For applications to a cylindrical geometry see D. Stigter.²⁹) The solution of the PB equation is considered to be a good approximation for the thermoelectrostatic potential around a macroion.⁹ However, it is the ionic distribution rather than the potential which is of ultimate interest to many molecular physical chemists. On the basis of this realization, we introduce the transformed Poisson–Boltzmann equations (TPB, eqs 9, below), which offer insight and analytical power by being expressed directly in terms of ionic distributions.

The PB and TPB equations are two mathematical formulations of the same physical theory. An advantage of the latter is that it makes the ionic distributions intuitively accessible, and many of the properties of most interest to an experimentalist are simply related to them. On the other hand, properties which are explicitly related to the potential such as electrophoresis and the free energy are best viewed from the point of view of the standard PB equation. Most of the results of the present work are general for a polyelectrolyte modeled as a very long

cylinder. However, because of our special interest, the numerical examples are mostly based on molecules with the dimensions and charge distribution of DNA. Among other things this means that our examples are concentrated on cases where the Manning charge density parameter $\xi > 1$, and in particular on the B-form DNA value of $\xi = 4.22$. Most of the results which are of direct interest to experimentalists will be found in the section on “The Excess Functions φ_{ct} and φ_{co} .”

The paper is developed as follows: 1. The notation, model and basic electrostatics are described and developed. 2. The charge distribution functions are defined and their differential equations derived. The condensation radius and a connection with the condensation theory as a limit are deduced. 3. Systems with no added salt are presented and explicitly solved for the three cases, $\xi < 1$, $\xi = 1$, $\xi > 1$. 4. The solutions for the PB equation are compared with the derivatives of the solutions for the TPB equation. 5. Numerical solutions for the case of added salt, the condensation radius and condensation limit for the salt-present case are obtained. 6. The excess functions φ_{ct} and φ_{co} are defined and derived from the numerical solutions of the TPB equations. Their direct relations with experimental quantities (Donnan exclusion, thermodynamic binding function, condensation) are derived and presented. Quantitative distinctions between the PB and condensation theories are discussed. 7. The dissociation radius, R_d ; and the accumulation of counterions and its relation to the Bjerrum theory of ion association are studied. 8. Major conclusions are summarized.

1. Notation and Background

The model for a polyelectrolyte will be the usual charged cylinder with length L and radius a . The cylinder is considered

[†] This paper is dedicated to Robert (Buzz) Baldwin in appreciation of years of fruitful interaction and friendship. The results of this paper were first presented in partial form at his retirement celebration in 1998.

* To whom correspondence should be addressed. E-mail: john@jas1.uoregon.edu.

[‡] E-mail: qian@amath.washington.edu.

to be sufficiently long that end effects can be ignored and is treated as a uniformly charged cylinder with uniform linear charge density, $z = Z/L$, where Z is the net number of fixed, elementary charges on the macromolecule. There are two classic cases. In the first there is no added salt and therefore no coions. All the counterions are in a finite cylinder with radius R , and the PB equation can be solved analytically.^{10,11} In the second case salt is present. A somewhat formidable analytical solution has recently been obtained for this case³¹ but most published work has made use of numerical integration of the differential equation. The situation with the TPB is completely analogous. The salt free case is solvable and numerical solutions will be used for the presence of salt.

In the presence of added salt the ionic atmosphere contains both counterions (ct) and coions (co). These subscripts are used rather than “+” or “−” to make the formulas independent of the sign of the charge on the polyion. The salt is assumed to be a 1:1 electrolyte. With the mean-field Boltzmann treatment local concentrations at a distance r from the cylinder axis are approximated as

$$n_{\text{ct}} = n_o e^y \quad \text{and} \quad n_{\text{co}} = n_o e^{-y} \quad (1)$$

where y is the reduced potential $y(r) = (e|\psi(r)|)/(kT)$, $\psi(r)$ is the mean electrostatic potential at r , and e is the protonic charge. y is always positive. n_o is the number density of the counterions at a distance r sufficiently remote from the polyelectrolyte that the presence of the polyelectrolyte is undetectable, and thus $y = 0$. For a 1:1 electrolyte this is same as the salt concentration far removed from polyelectrolyte molecules or the concentration of the salt in dialysis equilibrium with the polyelectrolyte solution.

With cylindrical symmetry and coordinates Poisson’s equation is

$$\nabla^2 \psi = \frac{1}{r} \frac{d}{dr} \left(r \frac{d\psi}{dr} \right) = -\rho/\epsilon$$

where ρ is the net charge density, in units of the elementary charge, resulting from counterions and coions. It is useful to introduce the dimensionless radial distance $x = r/l_D$ where $l_D = 1/\kappa$ is the Debye length and $\kappa^2 = (2e^2 n_o)/(\epsilon kT)$. Replacing r by x and ψ by y , Poisson’s equation takes the form²⁹

$$\frac{1}{x} \frac{d}{dx} \left(x \frac{dy}{dx} \right) = \frac{e^y - e^{-y}}{2} = \sinh y \quad (2)$$

Another characteristic length of importance is the Bjerrum length,

$$l_B \equiv e^2/4\pi\epsilon kT \quad (3)$$

It is the distance at which a pair of singly charged ions have an interaction free energy of kT . It arises automatically in calculations of ion distributions in solution. l_B is a function of the dielectric constant and temperature. For water at 25 °C its value is 7.13 Å.

We apply Gauss’ law to the surface of a cylinder, coaxial with the polyion, of radius r and length l , with $a \leq r \leq R$,

$$(2\pi l r) \frac{\partial \psi}{\partial r} = -\frac{Q}{\epsilon} = -\frac{l z(r) e}{\epsilon}$$

Q is the total charge contained in the cylindrical section of height

l and $z(r)$ is linear charge density, specifically the number of elementary charges per unit length (polyion plus the net charge of the ion atmosphere within the cylinder). Introducing the dimensionless potential and radius (y and x)

$$x \frac{\partial y}{\partial x} = -\frac{e^2 z(x)}{2\pi\epsilon kT} = 2l_B z(x) \quad (4)$$

The right side of eq 4 can be interpreted as minus twice the number of elementary charges contained in length l_B of the cylinder. In particular, at $r = a$, $x = x_a$

$$x_a \left(\frac{\partial y}{\partial x} \right)_{x_a} = -2l_B z(x_a) = -2\xi \quad (5)$$

where $\xi = e^2/(4\pi\epsilon kTb)$ is the dimensionless charge density discussed by Manning. $z(x_a)$ is often written as $1/b$, where b is the average charge separation. From this derivation we see that $\xi = l_B z(x_a)$ is the number of elementary charges that are contained in a Bjerrum length of the polyion.

2. Transformed Poisson–Boltzmann Equations

We will be mainly concerned with the ionic distributions around the polyion rather than the potential and it is therefore desirable to transform the PB equation to a form in which the unknown functions are the ionic distributions. We consider a cylindrical section of the ion atmosphere with a height of l_B extending from a to an outer limit R . In the case where there is no salt (no coion) R is the outer limit of the cylindrical volume surrounding the polyelectrolyte. This is the cell model. When salt is present R is chosen to be sufficiently remote that the ionic concentrations at R do not differ appreciably from their values at infinity where $y = 0$. This condition will be discussed further when actual calculations are presented.

Within the cylindrical section described above we define the cumulative quantity of ions between a variable radius r , $a \leq r \leq R$, and the external boundary at R . For the counterions this is given by

$$\Phi_{\text{ct}}(r) = 2\pi l_B \int_r^R n_{\text{ct}} r' dr' = 2\pi l_B n_o \int_r^R e^y r' dr'$$

Integrals of this form have appeared in the works of many authors especially for the case where r is equal to the radius of the cylinder to include the entire ionic atmosphere.^{2,16,15,21,29} From the above definitions of κ^2 and l_B we have $\kappa^2 = 8\pi l_B n_o$, so that the definition may be written as

$$\Phi_{\text{ct}}(r) = \kappa^2/4 \int_r^R e^y r' dr' = 1/4 \int_x^X e^y x' dx' \quad (6a)$$

where $X = \kappa R$. Similarly, for the coion

$$\Phi_{\text{co}}(r) = \kappa^2/4 \int_r^R e^{-y} r' dr' = 1/4 \int_x^X e^{-y} x' dx' \quad (6b)$$

Note that Φ_{ct} and Φ_{co} are positive irrespective of the charges on the ions.

We now find differential equations for these quantities. $\Phi_{\text{ct}} - \Phi_{\text{co}}$ is the magnitude of the net charge between the surfaces of r and R . Because of the overall neutrality of the system it is also the magnitude of the charge within r , i.e., the charge of the polyion plus the ionic atmosphere within r . From (4) and

(6a) we have

$$x \frac{dy}{dx} = -2(\Phi_{ct} - \Phi_{co}) \quad (7)$$

$$\frac{d\Phi_{ct}}{dx} = -\frac{1}{4}xe^y \quad (8)$$

taking the second derivative, $(d^2\Phi_{ct})/(dx^2) = -1/4(e^y + xe^y(dy)/(dx))$, and eliminating terms in y with eqs 7 and 8, we obtain the transformed PB equations

$$\frac{d^2\Phi_{ct}}{dx^2} = \frac{1 - 2(\Phi_{ct} - \Phi_{co})}{x} \frac{d\Phi_{ct}}{dx} \quad (9a)$$

and for Φ_{co}

$$\frac{d^2\Phi_{co}}{dx^2} = \frac{1 + 2(\Phi_{ct} - \Phi_{co})}{x} \frac{d\Phi_{co}}{dx} \quad (9b)$$

Equations 9 are a pair of coupled, nonautonomous, ordinary differential equations for Φ_{ct} and Φ_{co} . We note that in both cases it is the net charge density, $\Phi_{ct} - \Phi_{co}$, which controls the behavior of the functions. The boundary conditions at $r = a$ and $r = R$ (or $x = x_a$ and $x = X$) are

$$\begin{aligned} \Phi_{co}(x_a) &= N_s; \quad \Phi_{co}(X) = 0 \\ \Phi_{ct}(x_a) &= \xi + N_s; \quad \Phi_{ct}(X) = 0 \end{aligned}$$

Here N_s is the number of co- and counterions contributed by the neutral salt in the volume between a and R and ξ is the total charge on the ionic atmosphere, which balances the charge on the polyelectrolyte. Note that $\Phi_{ct}(x_a) - \Phi_{co}(x_a) = \xi$.

While the PB equation is derived by combining Poisson's equation (second order) and the Boltzmann law to the local ionic concentrations, the TPB equations arise from Gauss' law for a cylindrical distribution (first order), and the Boltzmann law to obtain cumulative distributions functions. Poisson's equation is, of course, the differential form of Gauss' law.

3. Counterion Distribution with No Added Salt

In the absence of additional salt there are no coions and it will be useful to write eqs 6a and 9a with r as a variable rather than x , since it will turn out that the results depend only on the ratios of distances and any scaling factor is automatically canceled. This can be seen by substituting αx for x in eqs 9a,b and observing the cancellation of α . The subscript for the counterions will be dropped in this section to distinguish it from the case with added salt, $\Phi_{ct} = \Phi$,

$$\Phi(r) = (k_{ct}^2/4) \int_r^R e^y dr \quad (6a)$$

$$\frac{d^2\Phi}{dr^2} = \frac{1 - 2\Phi}{r} \frac{d\Phi}{dr} \quad (10)$$

$$\Phi(a) = \xi; \quad \Phi(R) = 0$$

When additional salt is not present, k_{ct} is defined in terms of the counterion concentration at the outer boundary,¹⁶ i.e., as $k_{ct}^2 = (2e^2 n_{ct}(R)/(ekT))$.

We introduce the variable $\ln r^{10}$, and eq 10 becomes

$$\frac{d^2\Phi}{d \ln r^2} = 2(1 - \Phi) \frac{d\Phi}{d \ln r} \quad (11)$$

The first integral of eq 11 can be obtained by inspection

$$\frac{d\Phi}{d \ln r} = C - (\Phi - 1)^2 \quad (12)$$

There are three solutions to eq 12 depending on the sign and magnitude of C

$$\frac{1}{c_1} \tan^{-1} \frac{\Phi - 1}{c_1} = -\ln r + c_2, \quad C = c_1^2 < 0$$

$$\Phi - 1 = \frac{1}{\ln r + c_2}, \quad C = 0$$

$$\frac{1}{c_1} \coth^{-1} \frac{\Phi - 1}{c_1} = \ln r + c_2, \quad C = c_1^2 > 0 \quad (13c)$$

These results come from standard integral tables. It should be noted how more direct these solutions are than that for the PB equation itself.^{1,10} We now discuss three physical situations.

High Charge Density, $\xi > 1$. From its definition $d\Phi/d \ln r$ must always be negative. For $\xi > 1$, the value of $\Phi - 1$ passes through zero at a distance which we will call R_c in imitation of the R_M of LeBret and Zimm.¹⁶ If C is positive, the slope is positive in the neighborhood of R_c where $(\Phi - 1)^2 < C$. Consequently, C in eq 12 must be negative to maintain the negative slope and we require solution 13a which can be written as

$$\Phi = 1 - c_1 \tan(c_1(\ln r - c_2)) \quad (13a')$$

Since Φ is a continuous and monotonic function of $\ln r$, its range must lie on a single branch of the tangent function. c_1 and c_2 can be evaluated by numerically solving the two boundary equations $(1/c_1) \tan^{-1}(\xi - 1)/c_1 = -\ln a + c_2$ and $(1/c_1) \tan^{-1}(-1/c_1) = -\ln R + c_2$. This case is illustrated in Figure 1a for $\xi = 4.22$ (DNA) and $R/a = 100$.

The distance R_c at which $\Phi = 1$ has been called the condensation radius by Zimm and LeBret.³² In our analysis it shows up as an inflection point in the Φ vs $\ln r$ curve and will play a prominent role in the analysis of results. This is especially clear if we note that at $\Phi = 1$, $c_2 = \ln R_c$ and

$$\Phi = 1 - c_1 \tan(c_1(\ln(r/R_c))) \quad (14)$$

This is a negative tangent curve centered on the inflection point $(\ln R_c, 1)$ with positive curvature within the condensation radius and negative curvature on the outside. These regions correspond to the condensed and dissociable regions of the ion atmosphere as discussed by Zimm and LeBret.^{32,16} It would be of pedagogic interest to pursue these aspects of the problem with the present formalism, but we will not do so since this area has already been extensively discussed by the cited authors. We do wish to call attention to the fact that the condensation radius and the inner and outer ionic atmospheres are generated simply and automatically with the TPB formalism.

In the limit of $a \rightarrow 0$, our result can be related to the Manning condensation model.²⁰ In this case we have $\ln r \rightarrow -\infty$ in the neighborhood of the polyelectrolyte. The function Φ is bounded at both limits. For a smooth monotonic function to be bounded

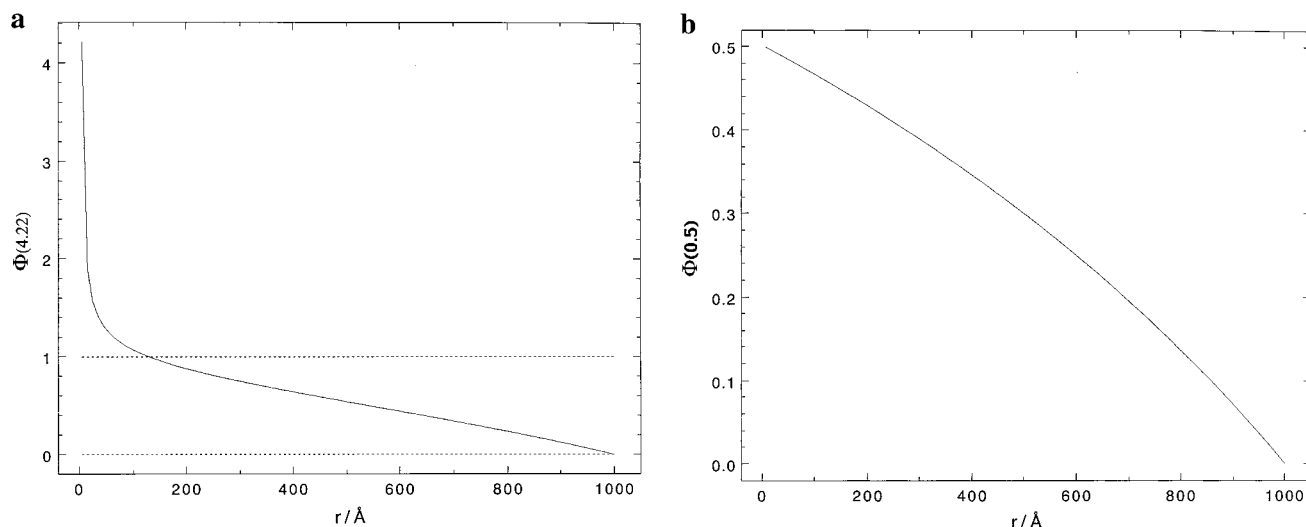


Figure 1. (a) The salt-free case. Plot of Φ vs r for $\xi = 4.22$, $A = 10$ Å, $R = 1000$ Å. R_c occurs where the unit line crosses the Φ curve. (b) Plot of Φ vs r for $\xi = 0.5$ and the same limits as in a.

at $-\infty$ it must have an asymptote parallel to the abscissa, i.e., $d\Phi/d \ln r = 0$. From eq 11 when $d\Phi/d \ln r = 0$, the second derivative also equals 0. From this we infer that in this limit the inflection point and therefore R_c , the condensation radius, has moved to the origin, or we might prefer to say that it is infinitesimally separated from it. This is a mathematical description of the Manning model. This type of conclusion has been obtained by others,^{17,12,16} but once again we emphasize the simplicity and directness of the present method. *This conclusion is reached without even solving the differential equation.*

We can look as well at the case for finite a and infinite dilution, i.e., $\ln R \rightarrow \infty$. Again Φ is bounded, the limiting slope must be zero, and the inflection point R_c moves to infinity. Mathematically, eq 11 is the same if we substitute $r' = r/R$, and $a' = a/R \rightarrow 0$. In our view these results are a matter of scaling. There are no zero or infinite boundaries. Material charges cannot be confined to a line. When R is fixed and $\ln a \rightarrow \infty$, we are adopting a macroscopic point of view. With this perspective the radius of the charge and R_c are both infinitesimally close to the z axis and we see only the negative curvature of the outer atmosphere. When a is fixed and $\ln R \rightarrow \infty$, the dissociable charges are concentrated in a shell at the outer edge of the cylindrical boundary, and on a molecular scale we see only the positive curvature of the condensed atmosphere. These are two viewpoints of the same problem when R/a is extremely large.

Low Charge Density, $\xi < 1$. In this case C can take on positive values provided that $C \equiv c_1^2 < (1 - \xi)^2$. From eq 13c the solution is

$$\Phi = 1 + c_1 \coth(c_1(\ln r + c_2)) \quad (13c')$$

The constants are evaluated from the boundary relations $(1/c_1) \coth^{-1}(\xi - 1)/(c_1) = \ln a + c_2$ and $(1/c_1) \coth^{-1}(-1/c_1) = \ln R + c_2$. The function is monotonic between $\ln a$ and $\ln R$, and there is no inflection point or accumulation of condensed ions. This is in agreement with all other studies. This function is shown in Figure 1b for $\xi = 0.5$, $r/a = 100$.

The Special Case, $C = 0$. From Eq 13b we have

$$\Phi = 1 + \frac{1}{\ln r + c_2} \quad (13b')$$

Applying the boundary condition $\Phi = 0$ at $r = R$, this becomes

$$\Phi = 1 - \frac{1}{1 + \ln(R/r)} \quad (14)$$

$\ln(R/r)$ is always positive so that Φ is always less than 1 except at $r \rightarrow 0$ where it becomes unity. We see that this case is appropriate for the special case of a line charge with $\xi = 1$. We note also that in the limit of $c_1 \rightarrow 0$ eq 13c becomes eq 13b'.

4. Solving the PB Equation.

There is naturally a great deal of overlap between the above results and those obtained by others using the PB equation. In fact the equations derived in the appendix of ref 16 are identical to the boundary conditions of our differential equation. One can easily obtain one set of solutions from the other. Equation 6a transforms from the potential to the ion distribution functions by an integration. The inverse is performed with a differentiation. From eq 6a

$$\frac{d\Phi}{d \ln r} = -\frac{(\kappa r)^2 e^y}{4}$$

and

$$y = \ln \left[\frac{-4}{(\kappa r)^2} \frac{d\Phi}{d \ln r} \right] \quad (15)$$

For $\xi > 1$ we differentiate eq 14 and substitute the result in eq 15

$$y = -2 \ln \left[\frac{(\kappa r) \cos(c_1(\ln r + c_2))}{2c_1} \right] \quad (16)$$

This is the solution to this problem reported by Alfrey et al.¹ For $\xi < 1$ differentiation of eq 13c' and substitution yields

$$y = -2 \ln \left[\frac{(\kappa r) \sin(c_1(\ln r + c_2))}{2c_1} \right] \quad (17)$$

This is the solution of Fuoss et al.¹⁰ for this case. Using the

TABLE 1: Coions within the Condensation Radius^a

C	R_c	$R_c - a$	$\Phi_{co}(<R_c)$	“fractional condensation” ^b
0.001	64.2	52.2	0.0046	0.764
0.003	49.6	37.6	0.0107	0.766
0.01	37.7	25.7	0.0269	0.769
0.03	29.7	17.7	0.0616	0.778
0.1	23.4	11.4	0.1502	0.799

^a $\xi = 4.22$; $a = 12$ Å; $\Phi_{co}(<R_c) = \Phi_{co}(a) - \Phi_{co}(R_c)$. ^b The condensation theory value is 0.763.

same procedure on eq 13b' for $\xi = 1'$

$$y = -2\ln\left[\frac{(\kappa r)(\ln r + c_2)}{2}\right] \quad (18)$$

This is the solution of ref 10 for this case apart from a factor of 2 which arises from a small difference in the definition of κ^2 .

Finally we can obtain a transformation formula between the potential and the charge distribution. Substituting eq 12 into eq 15

$$(\kappa r)^2 e^y = -4(C - (1 - \Phi)^2)$$

This permits one to calculate the potential from Φ and vice versa once the constants have been determined by either method. This formula is a generalization of a boundary condition derived in the appendix of ref 16.

5. The Ion Atmosphere in the Presence of Salt.

For this case we must consider the coupled differential equations for Φ_{ct} and Φ_{co} eqs 9a,b. First, however, we begin with a brief discussion of the properties of the Φ_{ct} function and its relation with the condensation concept. For the counterion we introduce the variable $\ln r$ to obtain the analogue of eq 11 in the presence of added salt.

$$\frac{d^2\Phi_{ct}}{d\ln r^2} = 2(1 - (\Phi_{ct} - \Phi_{co}))\frac{d\Phi_{ct}}{d\ln r} \quad (19a)$$

We note that at the r value for which $\Phi_{ct} - \Phi_{co} = 1$ there is an inflection point involving a change in sign of the second derivative. As discussed above, Zimm and LeBret³² and MacGillivray¹⁸ have introduced the idea of a condensation radius for the PB description of the ion atmosphere for cylindrical charge distribution of high density. For a polyelectrolyte of linear charge density ξ and no added salt, there are by definition $\xi - 1$ counterion charges within the radius R_c and one charge outside. These correspond to fractional charges of $(\xi - 1)/\xi$ and $1/\xi$ respectively. Similarly we define a condensation radius for the case of added salt. At R_c the net charge, $\Phi_{ct} - \Phi_{co}$, equals unity. The difference is that in the presence of salt there is a small fraction of coions within the condensation radius and a corresponding increase in the number of counterions. However, the last column in Table 1 indicates that the amount of coion in the condensation zone is quite small compared to the counterions. The inflection point in the Φ_{ct} vs $\ln r$ function is a very useful marker for locating this important boundary in the ion atmosphere of cylindrical polyelectrolytes.

The same arguments as in section 4 can be used to demonstrate the condensation-like behavior of the ion atmosphere when considering a line charge, $a \rightarrow 0$. In this case Φ_{ct} approaches the finite limit ξ as $\ln r \rightarrow -\infty$. The curve must have negative curvature at small $\ln r$ and zero slope and curvature in the limit. See Figure 3 below. This shows that the inflection

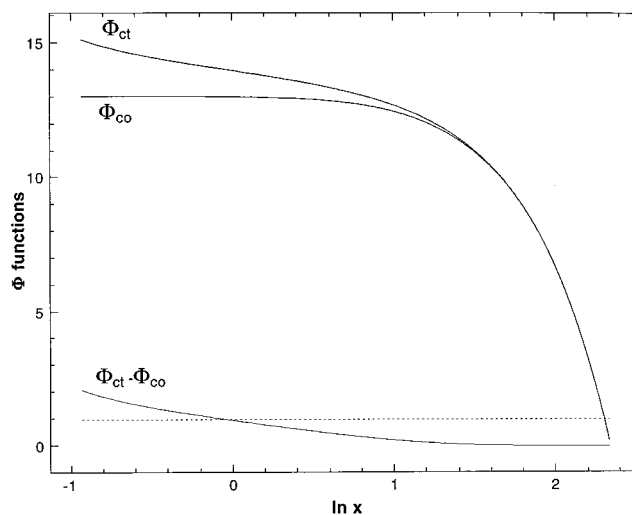


Figure 2. Plots of total counterion Φ_{ct} , total coion Φ_{co} , and net charge $\Phi_{ct} - \Phi_{co}$, for $\xi = 2.11$ and $C = 0.01$ M. $\ln x$ is the independent variable. Note inflection of Φ_{ct} curve occurs at $\Phi_{ct} - \Phi_{co} = 1$.

point, X_c , and therefore the condensation radius R_c , also approaches $-\infty$ so that the charge outside an infinitesimal region is one charge per Bjerrum length. Again, this is just a matter of scaling. In terms of the variable $\ln x = \ln \kappa r$ we have the same equation

$$\frac{d^2\Phi_{ct}}{d\ln x^2} = 2(1 - (\Phi_{ct} - \Phi_{co}))\frac{d\Phi_{ct}}{d\ln x} \quad (19b)$$

which introduces the natural scaling factor of the Debye length. We will use the notation $X_c = \kappa R_c$ to denote the condensation radius on the x scale. $\ln x \rightarrow -\infty$ now implies that the ionic strength is sufficiently low that a is infinitesimally small compared with $1/\kappa$. Though the “condensed” layer is infinitesimally thin on a macroscopic or semimacroscopic scale, it has the usual PB structure when looked at on the scale of molecular dimensions.

Equations 9a,b can be solved using the Runge–Kutta shooting method by introducing the variables $u = d\Phi_{ct}/dx$, $v = d\Phi_{co}/dx$ and integrating the resulting four coupled, linear differential equations.²² This is tedious work. It can be done by following D. Stigter’s procedure of assuming Debye behavior far from the polyelectrolyte molecule to obtain initial slopes at the distant point $x = X$ and then integrating the coupled equations. Doing this for a series of initial conditions gives results for a series of polyion charge densities. Interpolation then can be used to obtain results for a charge density of interest. Since we had at hand a program supplied by D. Stigter²⁹ for the accurate calculation of PB potentials for the cylindrical problem, it was much easier to simply evaluate $\Phi_{ct}(x)$ and $\Phi_{co}(x)$ directly by integrating eqs 6a,b using Simpson’s rule.^{22,p133} With the boundary condition $\Phi_{ct}(x_a) - \Phi_{co}(x_a) = \xi$, it was possible to check on the accuracy of the integration by comparing the value of $\Phi_{ct}(x_a) - \Phi_{co}(x_a)$, which resulted from the integrations with that of ξ , which was assumed at the starting point of the potential calculation. It was found that starting the integration at $X = 10$ gave results accurate to better than one part in 1000. $X = 12$ was thereafter used as a standard. On the other hand it is useful to compare cylinders which contain the same amount of added salt. With full tables of $\Phi_{ct}(x)$ and $\Phi_{co}(x)$ from the integrations it was easy to make slight adjustments of X for the various runs so that all systems contained the same amount of salt. This could be done without damaging the accuracy of the integrations.

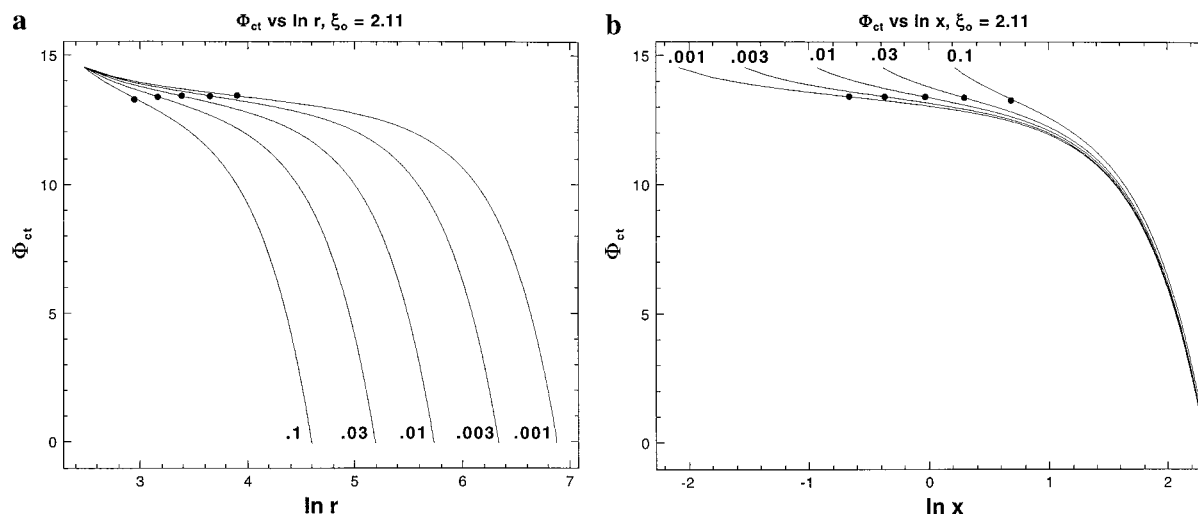


Figure 3. The effect of variation of salt concentration on R_c and X_c for $\xi = 2.11$. (a) The increase of R_c . (b) The decrease of X_c .

Typical results are shown in Figure 2. The polyelectrolyte charge density is 2.11 per Bjerrum length; the Debye length is 30.4 Å. The right sides of the two Φ curves ($r > 180$ Å) essentially coincide indicating that this region is beyond the ion atmosphere of the polyion. This is also indicated by the close to zero accumulated charge, $\Phi_{ct} - \Phi_{co} = 0$, in this region. (Actually 1% of the countercharge lies beyond 165 Å, 0.1% beyond 240 Å, 0.01% beyond 290 Å, and 0.001% beyond 310 Å.) The accumulated charge at the surface of the polyion ($a = 12$ Å) is 2.11 as it must be. The total number of ions in the selected region ($a \leq r \leq R$) is 15.13 for counterions and 13.02 for coions. Only the difference between these numbers has any significance since the position of the outer boundary is arbitrary as long as it is effectively beyond the polyion atmosphere. This arbitrariness will be removed in the next section when we consider only the excess ionic concentrations.

On the right side of the figure the curves form an inverted parabola which merely represents the volume of the cylindrical shell between r and R . Further to the left there is a Debye–Hückel region where the potential causes the curves to separate from one another, but is not yet large. Further to the left the potential is large leading to a strong accumulation of countercharge as predicted from the PB equation. This is represented not only by an increase in slope, but a change in curvature from negative to positive.

Results for Φ_{ct} as a function of $\ln r$ and ionic strength are shown in Figure 3a. The curves all converge to the same point at the boundary of the polyion. ($r = a = 12$ Å) The separation of the curve on the right represents the increasing values of R necessary to retain the same amount of salt in the outer cylinder. This increase goes very nearly as $1/\kappa$, (i.e., $1/\sqrt{C}$), when R/a is large. This set of curves simulates a dilution experiment. The heavy dots indicate the positions of the inflection points at R_c are located via the condition that $\Phi_{ct} - \Phi_{co} = 1$ at R_c . R_c increases with diminishing ionic strength but not so rapidly as R . We can compare this behavior with discussions by Le Bret and Zimm¹⁶ and Gueron and Weisbuch¹² who found that R_c for the salt free case varied as $1/\kappa$, where κ is defined in terms of the concentration of counterions within the enclosing outer cylinder. Numerical calculations by LeBret and Zimm indicate that the variation would be slower for the case of added salt. This is verified by the figure which shows that R_c varies considerably more slowly than R . Over the range of our calculations it varies roughly as $R_c = aC^{-0.21}$ where $a = 12$ Å.

We have not looked at its asymptotic dependence for extremely low salt concentrations.

Although R_c increases with decreasing ionic strength, the number of coions within it decreases regularly, as is shown in Table 1 which lists numerical values for R_c and the number of coion charges within R_c . The number of coions within R_c is easily calculated as $\Delta\Phi_{co} = \Phi_{co}(a) - \Phi_{co}(R_c)$ listed in column 4. Distance are in angstroms. $R_c - a$ represents the thickness of the cylindrical shell between the surface of the cylindrical polyion and R_c . In the absence of binding to the polyion surface, the total mobile charge within R_c is $\xi - 1 = 3.22$. $\Delta\Phi_{co}$ decreases as ionic strength is reduced and extrapolates to zero at zero ionic strength. It is very accurately described by a linear log–log relation. See Figure 4b.

Returning to the behavior of Φ_{ct} and Φ_{co} we see a different picture in Figure 3b which shows the same data plotted as a function of $\ln x$. Now the left termini of the curves are separated from one another because of the dependence of x_a on the ionic strength while the right termini almost coalesce since κR is almost independent of C (κ varies as \sqrt{C}) at constant salt, and R almost follows a cylindrical $1/\sqrt{C}$ dilution law.) Now we notice that X_c progressively decreases as the ionic strength decreases, Figure 4a. This is the behavior alluded to above where it was shown that as $\ln x \rightarrow \infty$, also $\ln X \rightarrow \infty$. Since, for a given r , x varies as $1/\sqrt{C}$, we have another demonstration that X_c increases more slowly than the Debye length as the salt concentration is decreased.^{16,17}

6. The Excess Functions φ_{ct} and φ_{co} .

Of more interest for practical purposes are the excess charge functions which are defined in terms of the excess concentrations of counterions and coions given by $n_{ct} - n_o = n_o(e^y - 1)$ and $n_{co} - n_o = n_o(e^{-y} - 1)$, respectively. In analogy to eqs 6 we have

$$\varphi_{ct}(x) = \frac{\kappa^2}{4} \int_r^R r(e^y - 1)dr = \frac{1}{4} \int_x^X x(e^y - 1)dx \quad (20a)$$

$$\varphi_{co}(x) = \frac{\kappa^2}{4} \int_r^R r(e^{-y} - 1)dr = \frac{1}{4} \int_x^X x(e^{-y} - 1)dx \quad (20b)$$

The position of the outer boundary at R , or $X = \kappa R$, is now immaterial provided it is sufficiently remote to contain essentially the entire ion atmosphere of the polyelectrolyte. Under

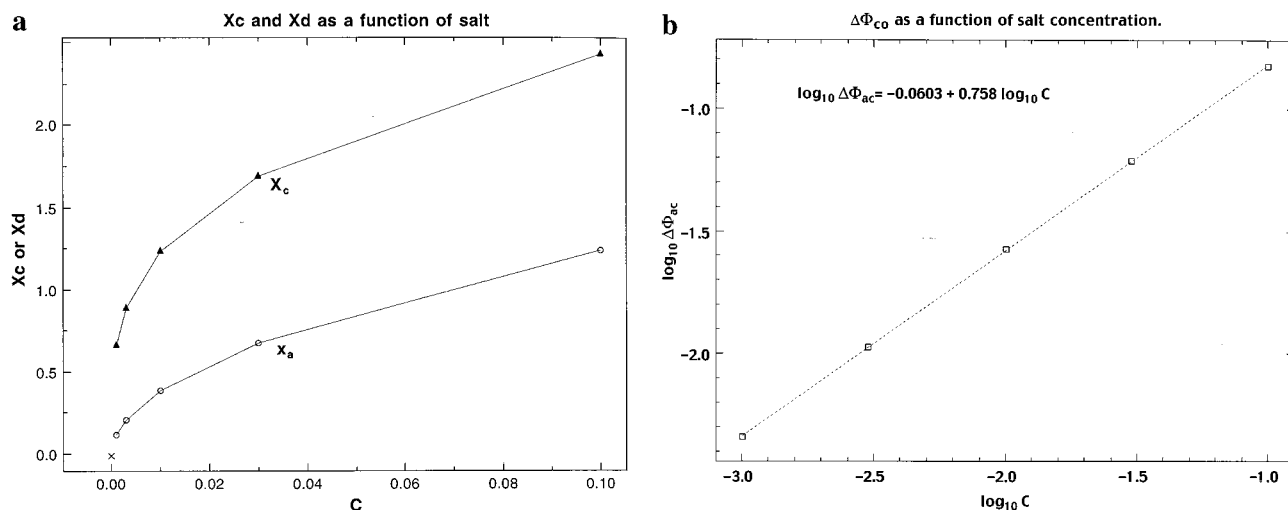


Figure 4. (a) X_c as a function of salt concentration. The limit point at (0,0) is known analytically as discussed in the text. (b) The amount of coion within the radius R_c as a function of salt. Under extreme dilution the near atmosphere about the polyelectrolyte is the same as for the salt free case.

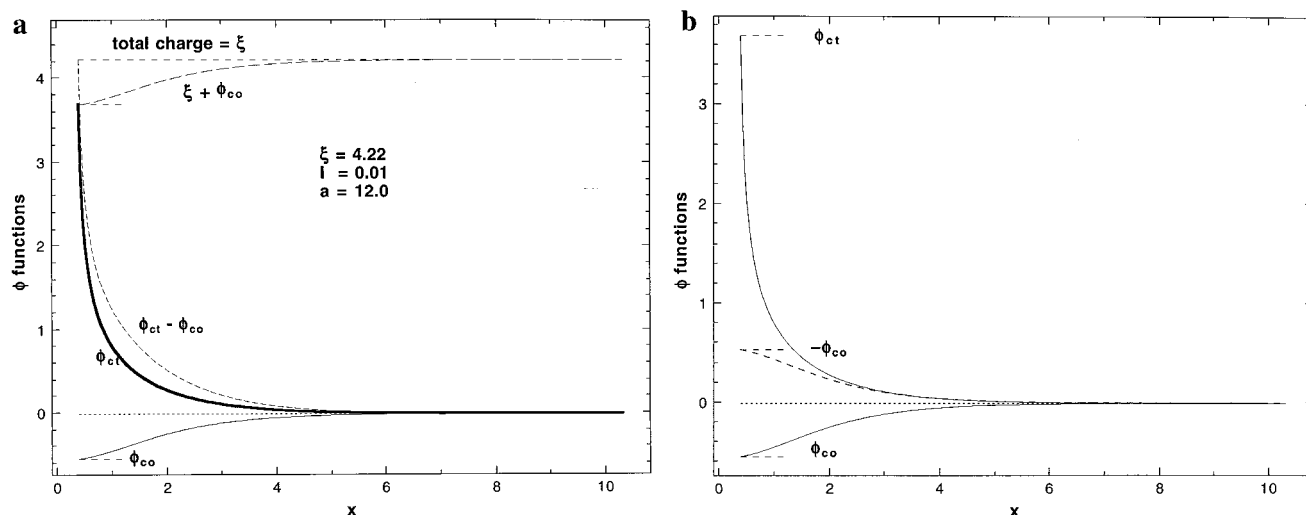


Figure 5. The excess functions ϕ_{ct} and ϕ_{co} . $\xi = 4.22$, $C = 0.01$ M. The heavy dark line is ϕ_{ct} and ϕ_{co} is always negative. Note that, at x_a , $\phi_{ct} = \xi + \phi_{co}$.

these conditions R or X is mathematically equivalent to an infinite boundary. The differential equations obeyed by these functions are

$$\frac{d^2\phi_{ct}}{dx^2} = \frac{1 - 2(\phi_{ct} - \phi_{co})}{x} \frac{d\phi_{ct}}{dx} + \frac{(\phi_{ct} - \phi_{co})}{2}$$

$$\frac{d^2\phi_{co}}{dx^2} = \frac{1 + 2(\phi_{ct} - \phi_{co})}{x} \frac{d\phi_{co}}{dx} + \frac{(\phi_{ct} - \phi_{co})}{2}$$

The boundary conditions are

$$\phi_{ct}(x_a) - \phi_{co}(x_a) = \xi \quad (21)$$

$$\phi_{ct}(X) \approx 0; \quad \phi_{co}(X) \approx 0 \quad \text{for sufficiently large } X$$

As in eqs 9, the behavior of the functions is determined by the net charge density of the atmosphere $\phi_{ct} - \phi_{co}$. We will not make direct use of these differential equations which have fewer revealing properties than those for the Φ functions. ϕ_{ct} and ϕ_{co} will be calculated directly by the numerical integration of eqs 20a and 20b using Stigter's program for calculating the potential. See the previous section. The result for a DNA molecule ($\xi =$

4.22; $a = 12$ Å) are shown in Figure 5a. Since the background concentrations of the neutral salt ions have now been removed, this figure deals with the net charges of the components of the ionic atmosphere. The short, horizontal dashed lines represent the extrapolated values of the functions at $r = a$. We note that the total charge of the ion atmosphere, $\phi_{ct}(a) - \phi_{co}(a)$, exactly compensates the charge on the cylinder, but the counterion charge is considerably less. This is an aspect of the Donnan effect. Thermodynamic equilibrium of the neutral salt takes place by the rejection of neutral salt from the near ionic atmosphere. This reduces the number of both counterions and coions by the same amount (Note the twin dashed curves descending to the left.) but obviously does not affect the charge of the ionic atmosphere. Since the neutral salt is the only source of coion, the salt rejection is given by $\phi_{co}(a)$ per ξ charges, which is negative. Integration over the ionic atmosphere to obtain the Donnan exclusion has of course been utilized by previous authors.^{11,21,28,29} On the usual per unit charge basis the Donnan coefficient is thus $\Gamma = \phi_{co}(a)/\xi$. Values for Γ as a function of salt concentration are given in Table 2. We note that $\phi_{ct}(a) = \xi + \phi_{co}(a) = \xi(1 + \Gamma)$. This exclusion of salt is related to the preferential interaction coefficient of the polyelectrolyte for the salt, $\Gamma = \partial C_3/\partial C_2$, where C is molar concentration, "3" stands for the salt component, and "2" for the polyelectrolyte.

TABLE 2: Donnan Exclusion and Counterion Release with the Poisson–Boltzmann Theory^a

C (ML ⁻¹)	Γ (PB) ^b	ψ^c
0.001	-0.096	0.808
0.003	-0.108	0.784
0.01	-0.127	0.746
0.03	-0.153	0.694
0.1	-0.196	0.608

^a $\xi = 4.22$; $\Gamma(\text{PB}) = \varphi_{\text{co}}/\xi$. ^b Gross and Strauss find $\Gamma = -0.059$ at extreme dilution which is identical with Manning's value from condensation theory. ^c From footnote b it is clear that the limiting value of ψ is the same for the condensation and Poisson–Boltzmann theory. For B-form DNA it is 0.886.²⁴

This is the electrostatic part of the exclusion. To this must be added the usual excluded volume C_3V_2 , where V_2 is the physical volume made unavailable by the presence of the polyelectrolyte molecule.^{11,29}

We wish now to compare the results of Figure 5 with the predictions of condensation theory in which we consider a Bjerrum-length segment to have a real charge of ξ but an effective charge of unity because of the condensation of $\xi - 1$ counterions. In the simplest type of discussion of the Donnan equilibrium (mass action formula, very small ratio of polyelectrolyte to salt, all activity coefficients unity) the salt exclusion equals half the polyelectrolyte charge. For a Bjerrum length of a polyelectrolyte we would have $\varphi_{\text{co}}(a) = -1/2$ and $\varphi_{\text{ct}}(a) = +1/2$, based on the effective charge. The Donnan exclusion per real charge is then $\Gamma = -1/(2\xi)$. This is the same result that one would obtain with the linear Debye–Hückel theory. Excess ion concentrations are proportional to y and $-y$ for the counterions and coions respectively so the excess concentrations are numerically equal but opposite in sign. These predictions are invalid when potentials are high.

A Curious Anomaly. G. Manning reminded us that he obtained $\Gamma = -1/(4\xi)$ from the limiting Debye–Hückel electrostatic free energy.²⁰ We have reproduced this result using another method based on the excess free energy. See the appendix for details. But if the number of excess coions is $\varphi_{\text{co}}(a) = -1/4$ per Bjerrum length, then the number of excess counterions must be $\varphi_{\text{ct}}(a) = +3/4$ to maintain electroneutrality. ($\xi - 1$ coions are condensed on the polyion.) This is a contradiction with the standard tenets of Debye theory which yields excess charges of opposite sign for coions and counterions.

We have come up with the following resolution. The nonlinear term in the cylindrical PB equation (eq 2) is \sinh which is an odd function of y . Expanding to obtain the linear Debye–Hückel equation should therefore be correct up to but not including third-order terms. On the other hand, the ionic concentrations are given by the exponential functions $e^{\pm y}$ and depend on second-order terms. There should therefore be a range of y values for which the equation for the potential remains accurate while the linear relation for the ionic concentrations becomes inaccurate. This perturbs the symmetry of the counterion and coion distributions while maintaining $\varphi_{\text{ct}}(a) + \varphi_{\text{co}}(a) = 1$ for the condensation case. We considered the possibility of using the potential obtained from the linear DH theory and retaining the second term of the expansion $e^{\pm y} - 1 = \pm y + y^2/2$ to determine the local concentrations. Substituting these expansions in eqs 20 gives the results

$$\varphi_{\text{co}}(a) = -1/4$$

$$\varphi_{\text{ct}}(a) = 3/4$$

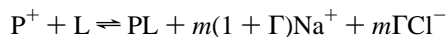
for the condensation case where the ξ_{eff} equals unity. Dividing by the real charge, ξ , we obtain $\Gamma = -1/(4\xi)$: Manning's result. The conclusion is that for the special case of condensation theory in the limit of low salt, consistency requires a hybrid form of the Debye–Hückel theory because of the high potential. The potential and quantities determined from it like the free energy are obtained from the linear PB equation. On the other hand the ionic distributions ($n_{\text{ct}}(r)$, $n_{\text{co}}(r)$, φ_{ct} , φ_{co}) require the quadratic terms to be consistent. In this case the usual Debye–Hückel symmetry is destroyed.

This result requires further study in the light of the following: (1) The quadratic expansion is in fact a poor representation of $e^{\pm y}$ at normal polyelectrolyte potentials. As a result the ratios of counterion to coion concentrations are much larger for the PB theory than for the quadratic approximation. (2) MacGillivray¹⁹ has concluded that the linear DH theory is a good approximation for $\xi < 1$. (3) The asymptotic value for Γ from the numerical solution of the PB equation is the same as that for the condensation theory in the limit of low salt.²⁰

We return to the PB results. Calculations similar to those shown in Figure 5 were performed as a function of 1:1 salt concentration and the results for the Donnan exclusion are shown in Table 2. We note that $|\Gamma|$ increases with ionic strength. Calculations which are not shown show also that it decreases with increasing charge density. The relatively wide variation of Γ as a function of salt concentration is one aspect in which the results of the PB theory disagree with those of the condensation theory. This variation has been observed experimentally.³⁰ Because of the constancy of the electrochemical potential, we have the mass action law $n_{\text{ct}}(r)n_{\text{co}}(r) = (n_0e^{y(r)})(n_0e^{-y(r)}) = n_0^2$. As a result, n_{ct} and n_{co} , as well as φ_{ct} and φ_{co} , are reciprocally related. The buildup of counterions near the polyion is large and varies with salt concentration and charge density. This change is reciprocally reflected in the Donnan exclusion. Despite these differences with the condensation theory it is of interest that the limiting value of the Donnan coefficient equals $-1/(4\xi)$ for both the PB theory¹¹ and condensation theory as was pointed out by Manning.²⁰

Another experimental quantity of considerable importance is the “counterion release” or “thermodynamic binding” discussed by Record et al. in a series of papers starting with ref 24 and summarized in ref 23. This quantity is a measure of the release of counterions from a polyelectrolyte like DNA when counterions are displaced from its surface by the binding of proteins or charged polypeptides (such as polylysine) or other polycations. The above authors initially made use of the condensation theory of Manning, and put their calculation in the context of the equilibrium binding of ligands to DNA. We wish to obtain an equivalent formula from a Poisson–Boltzmann formalism by investigating the consequences of effectively removing the charge density from a segment of a polyelectrolyte. This provides an expression for counterion release which can then be applied to binding equilibria. For simplicity we consider that the ligand L releases the ionic atmosphere associated with a Bjerrum length of the polyelectrolyte containing ξ charges. Longer or shorter lengths can be considered by a simple multiplication factor. Referring to Figure 5a, the number of counterions released when polyelectrolyte charges are eliminated from a segment of DNA of length l_b by neutralization or blockage is just $\varphi_{\text{ct}}(a) = \xi + \varphi_{\text{co}} = \xi(1 + \Gamma)$. In addition $|\varphi_{\text{co}}(a)| = \xi|\Gamma|$ moles of coion are moved from the external solution to the immediate neighborhood of the polyelectrolyte. Recall that Γ is negative. This can be looked at as a two step process. First, $|\varphi_{\text{co}}(a)|$ moles of salt are removed from the bulk

solution and introduced into the neighborhood of the polyion thereby raising $\varphi_{ct}(a)$ to ξ and $\varphi_{co}(a)$ to zero. Second, ξ counterions are released into the solution, giving a net release of counterion of $\xi + \varphi_{co}(a) = \varphi_{ct}(a)$. To put these quantities on the basis of the number of polyion charges eliminated or blocked by the ligand m , we must multiply by m/ξ . Obtaining $m(1 + \Gamma)$ and $m\Gamma$, respectively, for counter and coions. We consider the “reaction”



where for concreteness we assume that the salt is NaCl and the polyion negative. P^+ represents the polyion with its ionic atmosphere. The two terms on the right represent the $m(1 + \Gamma)$ released to the surroundings, a positive quantity, and the coions removed from the surroundings $m\Gamma$, a negative quantity. This leads to the equilibrium expression

$$K = \frac{[PL]}{[P]} [Na]^{m(1+\Gamma)} [Cl]^{m\Gamma} = K_{app} [Na]^{m(1+\Gamma)} [Cl]^{m\Gamma}$$

where K_{app} is the empirically observed ratio of occupied to unoccupied sites for the ligand. Since $[Na] = [Cl] = [S]$ outside the polyion atmosphere, where $[S]$ is the salt concentration, we have

$$K = K_{app} [S]^{m(1+2\Gamma)}$$

from which we obtain the well-known logarithmic relation²⁴

$$\log K = \log K_{app} + m(1 + 2\Gamma)\log[S] \quad (22)$$

Record et al.²³ define a function ψ which is the counterion release per unit charge of the polyelectrolyte. This is given by $\psi = 1 + 2\Gamma$, a result previously found by these authors.³ The slope in eq 22 is $m\psi$. The original derivation was applied to condensation theory with $\Gamma = -0.059$, so that $\psi = 1 - 1/(2\xi) = 0.882$.

ψ is a variable in the Poisson–Boltzmann theory. Values for B-form DNA are given in the last column of Table 2 as a function of ionic strength. As a result the coefficient of $\log[S]$ in eq 22 is a variable. Biophysical chemists have made much use of the slope of the $\log K_{app}$ vs $\log[S]$ plot to determine m , the number of charges covered or neutralized by a ligand as a measure of the ligand size. This technique has also been calibrated with ligands of known lengths and apart from some exceptional cases must be considered as a well-established method. We were concerned to note that the PB results did not seem to conform with eq 22 with a constant coefficient. Nevertheless when $\log[S]^{(1+2\Gamma)}$ is plotted vs $\log[S]$ with variable values of Γ taken from Table 2 and no assumption of a linear relation, a quite good straight line relationship is obtained with a coefficient of 0.91 in good agreement with the limiting condensation value of 0.88 and with the calibration experiments. The results are shown in Figure 6. This validates the method within the Poisson–Boltzmann model.

Polyelectrolyte and colloid chemists have long been aware of the accumulation of counterions near charged planar and cylindrical surfaces which does not obey the usual mass action dilution law, but in general have not applied a particular measure to the quantity or fraction of the counterions which are accumulated. On the other hand, the excess trapped or bound counterions play a prominent role in condensation theory.²⁰ We will attempt to define the quantity of condensed ion in a PB distribution. One way to do this is to assign all cations within the condensation radius as condensed ions. This is given by

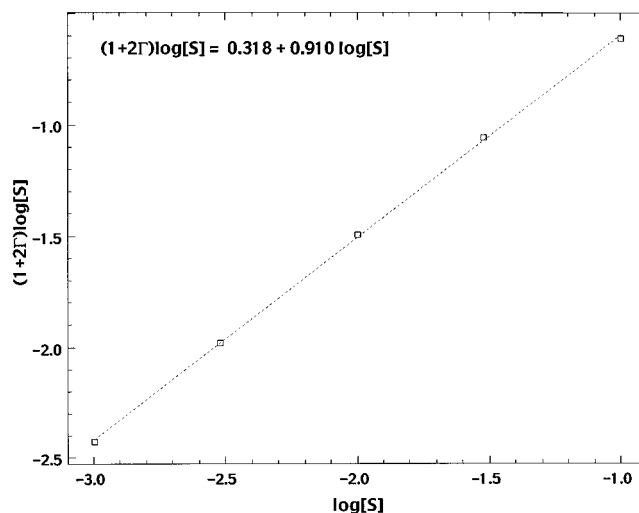


Figure 6. The salt dependence of log for thermodynamic binding to DNA utilizing the Poisson–Boltzmann theory. Note that though the log–log plot looks linear, the exponent of the salt concentration $(1 + 2\Gamma)$ is monotonically varying. See text and Table 2. The squares are calculated points. The dotted line is the least squares linear fit.

TABLE 3: Summary of Results^a

	φ functions	PB theory ^b (per unit charge)	condensation theory (per unit charge)
Donnan exclusion ^c	$\varphi_{co}(a)$	Γ	$-1/(4\xi)$
free counterion charge	$\xi + \varphi_{co}(a)$	$1 + \Gamma$	$3/(4\xi)$
counterion release ^c	$\varphi_{ct}(a) + 2\varphi_{co}(a)$	$1 + 2\Gamma$	$\psi = 1 - 1/(2\xi)$
polymer charge density ^c	$\varphi_{ct}(a) - \varphi_{co}(a)$	1	1
“condensation”	$\Phi_{ct}(a) - \Phi_{ct}(R_c)$	$(\xi - 1 + \Delta\varphi_{co})/\xi$	$\psi_c = (\xi - 1)/\xi$

^a In the limit quantities marked with an asterisk are identical in the PB and condensation ^bValues of Γ as in Table 2. ^c See Table 1.

$\varphi_{ct}(<R_c) = \Phi_{ct}(a) - \Phi_{ct}(R_c)$. See the discussion of of coions above. The net charge in the condensation zone is $\xi - 1$. It is also $\Delta\Phi_{ct} - \Delta\Phi_{co}$ so that $\Delta\Phi_{ct}$ may be obtained directly from the fourth column of Table 1. We have calculated the fractional condensation for DNA, defined as $\Delta\Phi_{ct}/\xi$, as a function salt concentration in the last column of Table 1. It never deviates too far from its condensation theory value of $(\xi - 1)/\xi = 0.763$.

Another way to define the extent of condensed ions is as the excess of counterions in the condensation zone over the coions. In this case the fractional condensation is exactly the same as in condensation theory since the number of charges of this excess must be precisely $\xi - 1$ since the remaining charges are exactly canceled by the charge of coions. The second definition has the advantage of simplicity and direct correlation with condensation theory. The first has the advantage of providing a picture of what is going on in the condensation zone as salt concentration is varied.

The experimental quantities associated with the ion atmosphere are the Donnan exclusion, the counterion replacement function ψ , the potential as determined by electrophoresis and ξ . The latter is often known a priori but is also obtainable from titration data or from electrophoresis.²⁸ Table 3 is a summary of the quantities discussed in this section together with their relation to experiment and to the condensation theory. In this section we have only touched on those aspects of polyelectrolyte thermodynamics which are simply connected to the ϕ and Φ

TABLE 4: Number of Counterions and Coions between $r = a$ and $r = R_d$

C	R_d	X_d	$\Phi_{ct}(<R_d)$	$\Phi_{co}(<R_d)$	$\varphi_{ct}(<R_d)$	$\varphi_{co}(<R_d)$
0.001	145.8	1.52	3.83	0.11	3.54	-0.18
0.003	96.2	1.73	3.86	0.14	3.49	-0.23
0.01	62.8	2.06	3.92	0.20	3.41	-0.31
0.03	43.9	2.50	4.03	0.31	3.30	-0.42
0.1	31.0	3.22	4.24	0.51	3.15	-0.57

distribution functions. For a more complete discussion, especially of recent work, see the review of Record et al.²³

7. Counterion “Binding” and Bjerrum Association.

It was shown above that the counterion accumulation function Φ_{ct} has an inflection point, $(d^2\Phi_{ct}/(d(\ln x)^2))_{x=X_d} = 0$. The inflection occurs at a distance R_c from the axis of the cylinder where R_c coincides with the condensation radius defined and analyzed by Zimm and LeBret. Φ_{ct} also has an inflection point in r (or x) space at a distance which will be symbolized as R_d and is related to dissociation. This may be seen from eq 9a which shows that the second derivative goes to zero when $\Phi_{ct} - \Phi_{co}$ equals $1/2$. Because of electroneutrality, the total charges inside and outside a cylinder of radius R_d are numerically equal to $1/2$ but opposite in sign.

The integrand of eq 9a is the distribution function for the counterions about the cylinder, so the condition, $((d^2\Phi_{ct})/(dx^2))_{x=X_d} = 0$, indicates that the distribution function, $xe^{y/4}$, has an extremum, actually a minimum, at R_d . The occurrence of a minimum in the distribution about spherical ions was noted many years ago by Bjerrum⁵ and was used by him to define electrostatic binding. All ions within the radius which we call R_d , for dissociation radius, are considered to be bound, those outside the radius to be dissociated. (R_d for the spherical case and monovalent ions is simply $l_b/2$ at standard temperature.) This concept was extensively used by R. M. Fuoss and C. A. Kraus for electrolytes dissolved in nonaqueous solvents.¹³

Kotin and Nagasawa noted the minimum in the PB counterion distribution for charged cylinders and used it to define a characteristic radius which is identical to our R_d .¹⁵ They suggested that the thermodynamic anomalies of polyelectrolytes could be explained in terms of the Bjerrum theory by assuming that all ions within this radius are bound. This idea was pursued later by Gross and Strauss,¹¹ who discussed the ideas of Kotin and Nagasawa in the context of their own PB calculations. Both groups dealt with the limiting case of extremely low salt to which we will return later.

The number of counterions and coions within R_d is easily evaluated in terms of the ionic distribution functions $\Phi_{ct}(<R_d) = \Phi_{ct}(a) - \Phi_{ct}(R_d)$ and $\Phi_{co}(<R_d) = \Phi_{co}(a) - \Phi_{co}(R_d)$. Compare with the condensation discussion in section 6. The results for DNA, $\xi = 4.22$, are presented in Table 4 as a function of salt concentration. The fixed total charge within R_d leads to the relation $\xi - \Phi_{ct}(<R_d) + \Phi_{co}(<R_d) = 0.5$ so that for DNA the fourth column minus the fifth column always equals 3.72, i.e., $\xi - 0.5$. The number of coions within R_d decreases as the salt concentration is decreased and approaches zero only at extreme dilutions (ca. 10^{-6} M). The variation with salt of the number of counterions within R_d is the result of increased diffusion of neutral salt into the region bounded by R_d .

Since at high salt concentrations a significant number of counterions lies within the radius R_d even in the absence of polyelectrolyte charge, it is appropriate to define binding as the excess over the background concentration, i.e., via the function $\varphi_{ct}(<R_d) = \Phi_{ct}(a) - \varphi(R_d)$. The value of $\Phi_{ct}(<R_d)$ actually exceeds the polyion charge in 0.1 M salt. It has been shown

that the uniform distribution of ligands in the absence of attractive or repulsive forces does not lead to any thermodynamic consequences.^{26,27} This function is given in the sixth column of Table 4. It is seen to be a variable in the PB theory and has a range from 75 to 84% of the polyion charge over the given range of salt concentrations. The source of the variation is the amount of coion charges within R_d , and this depends on the fraction of the Donnan exclusion contributed by the inner association region.

In the presence of salt we could also define the Bjerrum binding as the excess counterion over that required to cancel the charge of the coions, i.e., $\Phi_{ct}(<R_d) - \Phi_{co}(<R_d)$. This gives the invariant answer of $\xi - 1/2$, or $1 - 1/(2\xi)$ on a per charge basis. This coincides with the condensation expression for counterion release, but the connection is not simple. The Bjerrum theory deals only with the population of counterions within a free energy barrier which is only a fraction of the ionic atmosphere. Thermodynamic binding is related to the entire atmosphere and involves the coions and Donnan exclusion. In fact, if it is postulated that the charge inside a cylindrical region is $1/2$ and that the charge arises only from excess counterions, then the number of excess counterions must be $\xi - 1/2$.

Kotin and Nagasawa considered the case where only counterions were within R_d , so that their argument was limited to extreme dilutions. In this case, with no coions inside the dissociation zone, the number of bound counterions is $\xi - 1/2$. This is the special case of the preceding paragraph. Gross and Strauss took up the Bjerrum idea in a somewhat different way to discuss their calculations of the Donnan exclusion. They assumed a Debye atmosphere outside R_d . At the time of their paper neither condensation nor the condensation radius had been put on a quantitative basis.

It appears to us that the Bjerrum theory is an important interpretive tool because it introduces a free energy barrier between a region which is dominated by electrostatic interaction (bound ions) and a region which is dominated by the entropy of dilution from this region. The Bjerrum association is variable because of the penetration of coions into the association zone. Bjerrum did not consider this problem for two reasons. The first was that he derived his value of R_d from Coulomb's law rather than with a screened potential so that coions did not come into the problem. By contrast the PB and TPB equations are governed by the total charge distribution and automatically introduce screening by ions of both charges. Second, Bjerrum was initially considering spherical ions in aqueous solution where R_d is 3.6 Å so that random penetration by ions of like sign is quite unlikely at normal concentrations.

8. Summary of Conclusions.

It should be recalled that in this paper the functions ξ , Φ , and φ refer to charges per Bjerrum length of cylindrical polymer.

1. For the salt-free case the transformed PB equation is easily solved, much more so than the standard differential equation for the potential. The solutions divide naturally into the cases $\xi < 1$, $\xi = 1$, and $\xi > 1$. For $\xi > 1$ the radius at which $\Phi_{ct} = 1$ occurs at R_c , the condensation radius introduced by LeBret and Zimm, and is an inflection point in a plot of Φ_{ct} vs $\ln r$.

2. For the salt free case, increasing the distance of the outer boundary R causes R_c to increase without limit, but $R_c/R \rightarrow 0$ in agreement with the results of LeBret and Zimm. If r is scaled by the Debye length, $x = \kappa r$, $X_c = \kappa R_c$, then $\ln X_c$ and the inflection point move to minus infinity on the log scale. This may be shown analytically by considering the limiting properties of Φ_{ct} and its derivatives or by actual calculation. These results

imply that in finite regions Φ_{ct} behaves as if there is a cylinder of infinitesimal radius at $x = 0$ with a charge density $\xi = 1$ per Bjerrum length. This provides a link with the condensation theory.

3. Also in the presence of salt an inflection point occurs at a radius within which the total charge, $\Phi_{ct} - \Phi_{co}$, equals unity. This is used to define a radius R_c (or X_c) which contains a charge of unity comprised in general of the polymer charge, counterions and coions. A consideration of the limiting properties of eqs 19b shows that the inflection point at $\ln X_c$ moves to $-\infty$, establishing again a link to the condensation theory, this time for the presence of salt. The number of coions within X_c goes to zero at infinite dilution. Figure 4a.

The advantage of the Φ functions is that they illustrate the competition between dilution at large distances and accumulation close to the polyion charge. The excess functions φ_{ct} and φ_{co} , on the other hand, tend to be directly related to experimental quantities. These relationships are summarized in Table 3.

4. φ_{co} is always negative, and since it is a direct measure of the change in salt, concentration caused by the polyelectrolyte, its value at the surface of the cylinder $\varphi_{co}(a)$ may be equated to the amount of Donnan exclusion. Donnan exclusion is normally evaluated on a per unit charge basis, so we have $\Gamma = \varphi_{co}(a)/\xi$. $|\Gamma|$ is an increasing function of ionic strength. In the PB theory, Table 2, whereas in condensation theory all the Donnan exclusion occurs in the Debye–Hückel atmosphere around a linear charge density of $1/\xi$, and has the constant value of $|\Gamma|$, which is the same as the limit of the PB theory at extreme dilution. The increase in $-1/(4\xi)$ with increasing ionic strength has been observed experimentally.³⁰ Our calculations of the Donnan exclusion agree with those of Gross and Strauss and of Stigter^{28,29} where they overlap.

5. $\varphi_{ct}(a) - \varphi_{co}(a)$ represents the entire charge of the ionic atmosphere and for electroneutrality must be numerically equal to the charge of the polyelectrolyte cylinder, $\varphi_{ct}(a) - \varphi_{co}(a) = \xi$.

6. $\varphi_{ct}(a) + \varphi_{co}(a) = \xi(1 + 2\Gamma)$, the number of bound counterions which are released when charges are neutralized or blocked (thermodynamic binding), is an important experimental quantity.²⁴ It equals the net number of counterions released to the atmosphere $\varphi_{ct}(a) = \xi(1 + \Gamma)$, plus the contribution of coions going the other way, i.e., $\varphi_{ct}(a) + \varphi_{co}(a) = \xi(1 + 2\Gamma)$. On a per unit charge basis the thermodynamic binding function is $\psi = (1 + 2\Gamma)$, a relation that was previously derived by analytical methods by Anderson and Record.⁴ Condensation theory assigns Γ the value $-1/(4\xi)$ leading to $\psi = 1 - 1/(2\xi)$ and the canonical value of 0.88 for DNA. (Table 2) Despite the variable exponent the dependence of binding equilibrium on $\log[S]$ is essentially linear for the PB theory and has a slope quite close to the condensation value, Figure 6.

7. **Condensed Counterions.** We have defined condensed ions as those which are contained within the condensation radius. For the salt-free case, the fraction condensed is $\psi_c = (\xi - 1)/\xi$ in agreement with condensation theory. In the presence of salt, the number of counterions within R_c is variable depending on the quantity of coion present in the condensation zone but it does not drift too far from the condensation value, Table 1.

8. **Bjerrum Association.** There is an inflection point in the φ_{ct} vs r curve which occurs when the net charge outside the boundary $\varphi_{ct} - \varphi_{co}$ equals $1/2$. At this point the counterion concentration is a minimum. This occurs at a distance, R_d , which we call the dissociation radius because of its connection with the Bjerrum theory of ion association. This connection has been made previously.¹⁵ Within this boundary attractive Coulomb

forces dominate and the ions may be considered to be bound. Outside the boundary diffusive forces (entropy) dominate. This concept presents an important mechanistic picture of ion association near highly charged polyelectrolytes, but it is not directly connected with thermodynamic binding which is a composite process that depends also on coion displacement and Donnan exclusion.

Acknowledgment. We thank Howard Reese, Dirk Stigter, and Bruno Zimm for many helpful discussions; H.Q. thanks Professors Marshall Fixman and Joel Lebowitz for correspondence in the early stage of this work. We thank Gerald Manning for profitable interaction concerning the condensation theory in section 6. After the submission of our manuscript we learned of a paper⁷ dealing with similar problems as our own. There is a remarkable parallel between the two papers, both of which extend the interpretation of the inflection point (Figure 2) to the case with added salt. Both make use of the integrated charge density functions and point out the significance of the inflection point with $\ln r$ as coordinate. While the work of Deserno et al. is focused on the cell model, we have emphasized in this paper the experimentally more relevant case of excess salt. We are currently working on an analysis which bridges these two special cases.

Appendix

Debye–Hückel and Condensation Calculations. For condensation calculations, we must distinguish between ξ_o , the true charge density of the polyion (possibly including bound charges), and ξ_{eff} , the effective charge after condensation. Hill has derived the formula for the electrostatic free energy of a cylindrical polyion in the Debye–Hückel approximation.¹⁴ In modern notation it may be written as²⁸

$$\mu_{el}/kT = \frac{\xi_{eff}K_o(x_o)}{x_oK_1(x_o)} \quad (A1)$$

The Donnan exclusion equals the preferential interaction coefficient for the salt component.

$$\Gamma_{23} = -\frac{1}{\xi_o} \left(\frac{\partial \mu_3}{\partial \mu_3} \right) = -\frac{1}{\xi_o} \frac{\partial \mu_{el}/kT}{\partial \ln a_3} \quad (A2)$$

Division by ξ_o leads to Donnan exclusion per unit polyion charge. Substituting eq A1 into eq A2, we obtain

$$\Gamma_{23} = -\frac{\xi_{eff}}{2\xi_o} \left(1 - \frac{\xi_{eff}}{2} \right) \left(1 - \left(\frac{K_o(x_o)}{K_1(x_o)} \right)^2 \right) \left(1 + m_3 \frac{\partial \ln \gamma_3}{\partial m_3} \right)^{-1} \quad (A3)$$

The last factor arises from the nonideality of the salt.⁸ At very low salt concentration (limiting conditions) the last two factors are unity. Putting $\xi_{eff} = 1$ for the condensation calculation we obtain $\Gamma_{23} = -1/(4\xi_o)$, which is Manning's result.

An alternative way to calculate Γ_{23} is by integrating over the atmosphere.²⁹ For the usual Debye–Hückel case with $e^{\pm y} - 1 = \pm y$,

$$\Gamma_{23} = \varphi_{co}(a)/\xi_o = -\frac{1}{4\xi_o} \int_{x_o}^{\infty} yx \, dx, \quad \text{with} \quad y = 2\xi_{eff} \frac{K_o(x_o)}{x_oK_1(x_o)} \quad (A4)$$

This integrates to

$$\Gamma_{23} = -\frac{\xi_{\text{eff}}}{2\xi_0} \left(1 - \frac{XK_1(X)}{x_0 K_1(x_0)} \right). \quad (\text{A5})$$

For large X and $\xi_{\text{eff}} = 1$

$$\Gamma_{23} = -1/(2\xi_0)$$

This does not agree with the result obtained with the free energy formula.

We now assume that the linear equation is adequate for y and the free energy, but that the expansion for the ionic concentrations must be carried out to the second term, $e^{\pm y} - 1 = \pm y + y^2/2 \pm$ (see text.) We obtain, instead of eq A4,

$$\Gamma_{23} = \frac{1}{4\xi_0} \int_{x_0}^X (-y + y^2/2) x dx = -\frac{\xi_{\text{eff}}}{2\xi_0} + \frac{1}{2\xi_0} \left(\frac{\xi_{\text{eff}}}{x_0 K_1(x_0)} \right)^2 \int_{x_0}^X x K_0^2(x) dx \quad (\text{A6})$$

Assuming the limiting case of $x_0 \rightarrow 0$, $x \rightarrow \infty$

$$\Gamma_{23} = -\frac{\xi_{\text{eff}}}{2\xi_0} \left(1 - \frac{\xi_{\text{eff}}}{2} \right) \quad (\text{A6})$$

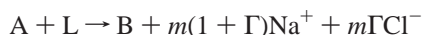
which again is Manning's result, $-1/(4\xi_0)$ for $\xi_{\text{eff}} = 1$. We note that to obtain this result we must conclude that the Debye–Hückel atmosphere is not symmetric: $\varphi_{\text{co}} = -1/4$; $\varphi_{\text{ct}} = 3/4$.

Counterion Release We derive the formula for counterion release including the displacement of coions in the opposite direction. The work is simplified by adopting a scheme for defining components suggested by Scatchard²⁵ and by Casassa and Eisenberg.⁶ When a polyion is added to a solution in osmotic equilibrium with a salt, what is added to the solution is not Na_2P , but Na_2P plus $Z\Gamma$ moles of salt because of Donnan exclusion. P is a polyion of charge Z and we assume that the salt is NaCl for concreteness. Recall that Γ is usually negative. The above authors suggest we treat the combined polyanion and salt as the component with the formula $\text{Na}_{Z(1+\Gamma)}\text{PCL}_{Z\Gamma}$. Gibbs long ago suggested that the choice of components in a system is arbitrary provided that the components are independent and sufficient. We define two polyanion components

$$A = \text{Na}_{Z(1+\Gamma)}\text{PCL}_{Z\Gamma}$$

$$B = \text{Na}_{(Z-m)(1+\Gamma)}\text{PCL}_{(Z-m)\Gamma}$$

A is the component discussed above, B is the component resulting from the addition of a ligand which displaces m charges from A when it is bound,



Note that the formula takes into account not only the release of m counterions, but also the adjustment of the Donnan exclusion to match the new charge on the polyion. A need not be free of ligand. Binding must be sparse, however. Otherwise binding statistics must be considered. At equilibrium

$$0 = \mu_B + m(1 + \Gamma)\mu_{\text{Na}} + m\Gamma\mu_{\text{Cl}} - \mu_A - \mu_L$$

This is converted into an equilibrium expression in the usual way

$$\ln K = \ln \left\{ \frac{[B]}{[A][L]} [\text{Na}]^{m(1+\Gamma)} [\text{Cl}]^{m\Gamma} \right\}$$

The apparent equilibrium constant is defined as $K_{\text{app}} = ([B])/([A][L])$ and $[\text{Na}^+] = [\text{Cl}^-] = [S]$ where $[S]$ is the salt concentration. So

$$\ln K = \ln K_{\text{app}} + m(1 + 2\Gamma) \ln [S]$$

$(1 + 2\Gamma)$ is the function called ψ by Record and co-workers.²⁴ For the condensation case $\Gamma = -1/(4\xi)$, as we have seen, so $\psi = 1 - 1/(2\xi)$ for this limiting case. See Table 3. In the PB theory Γ is a variable and this was taken into account in the construction of Figure 6.

For a consideration of the effect of ligand charge, length of polyelectrolyte, binding statistics, etc., see references of Record's group.²³

Glossary

- ct, co = counterion, coion
- b = reciprocal of z
- C = concentration, mol/L
- l_b = Bjerrum length. See eq 3
- n_o = ionic number density, ions/mL
- $n_{\text{ct}}(r)$, $n_{\text{co}}(r)$ = number of densities of counter- and coions
- R_c = condensation radius
- R_d = association radius
- X_c = reduced condensation radius
- X_d = reduced association radius
- y = reduced electrostatic potential
- z = charges per unit length on polyion
- Γ = preferential interaction coefficient, per unit charge
- κ = reciprocal of Debye length
- ξ = Manning–Oosawa reduced charge density
- Φ_{ct} , Φ_{co} = cumulative charges. See eqs 6
- φ_{ct} , φ_{co} = cumulative excess charges. See eqs 20
- ψ = electrostatic potential

References and Notes

- (1) Alfrey, T.; Berg, P. W.; Morawetz, H. *J. Polym. Sci.* **1951**, 7, 543–547.
- (2) Anderson, C. F.; Record, M. T. *Biophys. Chem.* **1980**, 11, 353–360.
- (3) Anderson, C. F.; Record, M. T. *J. Phys. Chem.* **1993**, 97, 7116–26.
- (4) Anderson, C. F.; Record, M. T., Jr. *J. Phys. Chem.* **1993**, 97, 7116–26.
- (5) Bjerrum, N. Investigations on Association of Ions, I. In *Niels Bjerrum Selected Papers*; Munksgaard: Copenhagen, 1926; pp 108–19.
- (6) Casassa, E. F.; Eisenberg, H. *J. Phys. Chem.* **1960**, 64, 753–756.
- (7) Deserno, M.; Holm, C.; May, S. *Macromol.* **2000**, 33, 199–206.
- (8) Eisenberg, H. *Biological Macromolecules and Polyelectrolytes in Solution*; Clarendon: Oxford, 1976.
- (9) Fixman, M. *J. Chem. Phys.* **1979**, 70, 4995–5005.
- (10) Fuoss, R. M.; Katchalsky, A.; Lifson, S. *Proc. Natl. Acad. Sci. U.S.A.* **1951**, 37, 579–589.
- (11) Gross, L. M.; Strauss, U. P. Interactions of polyelectrolytes with simple electrolytes. 1. Theory of Electrostatic Potential and Donnan Equilibrium for a Cylindrical Rod model: The Effect of Site Binding. In *Chemical Physics of Ionic Solutions*; Conway, B. E., Barradas, R. G., Eds.; Wiley: New York, 1966; pp 361–389.
- (12) Gueron, M.; Weisbuch, M. *Biopolymers* **1980**, 19, 353–382.
- (13) Harned, H. S.; Owen, B. B. *The Physical Chemistry of Electrolyte Solutions*; Reinhold: New York, 1950.
- (14) Hill, T. L. *Arch. Biochem. Biophys.* **1955**, 57, 229–239.
- (15) Kotin, L.; Nagasawa, M. *J. Chem. Phys.* **1962**, 36, 873–879.
- (16) Le Bret, M.; Zimm, B. H. *Biopolymers* **1984**, 23, 287–312.
- (17) MacGillivray, A. D. *J. Chem. Phys.* **1972**, 56, 83–5.

- (18) MacGillivray, A. D. *J. Chem. Phys.* **1972**, *56*, 80–3.
- (19) MacGillivray, A. D.; Winkleman, J. J. *J. Chem. Phys.* **1966**, *45*, 2184–2188.
- (20) Manning, G. S. *J. Chem. Phys.* **1969**, *51*, 924–33.
- (21) Ni, H.; Anderson, C. F.; Record, M. T., Jr. *J. Phys. Chem. B* **1999**, *103*, 3489–3504.
- (22) Press, W. H.; Teukolsky, S. A.; Vetterling, W. T.; Flannery, B. P. *Numerical Recipes*; Cambridge University Press: Cambridge, 1992; p704ff.
- (23) Record, M. T., Jr.; Zhang, W.; Anderson, C. F. *Adv. Protein Chem.* **1998**, *51*, 281–353.
- (24) Record, M. T.; Lohman, T. M.; de Haseth, P. *J. Mol. Biol.* **1976**, *107*, 145–158.
- (25) Scatchard, G.; Bregman, J. *J. Am. Chem. Soc.* **1959**, *81*, 6095.
- (26) Schellman, J. A. *Biopolymers* **1987**, *26*, 549–559.
- (27) Schellman, J. A. *Biophys. Chem.* **1990**, *37*, 121–140.
- (28) Schellman, J. A.; Stigter, D. *Biopolymers* **1977**, *16*, 1415–34.
- (29) Stigter, D. *J. Colloid Interface Sci* **1975**, *53*, 296–306.
- (30) Strauss, U. P.; Helfgott, C.; Pink, H. *J. Phys. Chem.* **1967**, *71*, 2550–2556.
- (31) Tracy, C. A.; Widom, H. *Physica* **1997**, *A244*, 402–13.
- (32) Zimm, B.; Le Bret, M. *J. Biomol. Struct. Dyn.* **1983**, *1*, 461–470.